AGU100 ADVANCING EARTH AND SPACE SCIENCE

Geophysical Research Letters

RESEARCH LETTER
10.1029/2019GL084948

The Possible Transition From Glacial Surge to Ice Stream on Vavilov Ice Cap

Whyjay Zheng[1], **Matthew E. Pritchard**[1], **Michael J. Willis**[2,3], **and Leigh A. Stearns**[4]

[1]Department of Earth and Atmospheric Sciences, Cornell University, Ithaca, NY, USA, [2]Cooperative Institute for Research in Environmental Sciences, University of Colorado Boulder, Boulder, CO, USA, [3]Department of Geological Sciences, University of Colorado Boulder, Boulder, CO, USA, [4]Department of Geology, The University of Kansas, Lawrence, KS, USA

Key Points:
- Outlet glacier at Vavilov Ice Cap displayed a new regime of ice dynamics in 2017, several years after an initial surge phase
- The transition indicates possible ice stream formation from the analyses of shear margin development, speeds, and Péclet number
- Multiple summer speedups are identified since 2015 and their strength correlates with warmer air temperature

Supporting Information:
- Supporting Information S1
- Table S1
- Table S2
- Movie S1

Correspondence to:
W. Zheng,
wz278@cornell.edu

Citation:
Zheng W., Pritchard, M. E., Willis, M. J., & Stearns, L. A. (2019). The possible transition from glacial surge to ice stream on Vavilov Ice Cap. *Geophysical Research Letters*, *46*. https://doi.org/10.1029/2019GL084948

Received 10 AUG 2019
Accepted 15 NOV 2019
Accepted article online 21 NOV 2019

Abstract Surge-type glaciers typically undergo cyclical flow instability due to mass accumulation; however, some recent glacier surges have caused irreversible ice loss in a short period. At Vavilov Ice Cap, Russia, surge-like behavior initiated in 2013 and by spring 2019 the ice cap had lost 9.5 Gt of ice (11% mass of the entire basin). Using time series of surface elevation and glacier velocity derived from satellite optical and synthetic-aperture radar imagery, we identify a shift of flow pattern starting in 2017 when shear margins formed within the grounded marine piedmont fan. Multiple summer speedups correlate with warmer summers during 2015–2019 and suggest that surface melt may access the subglacial environment. Force balance analysis and examination of the Péclet number show that glacier thinning propagated upstream in 2016–2017, and diffusion became a significant dynamic response to thinning perturbations. Our results suggest that the glacier has entered a new ice stream-like regime.

Plain Language Summary A glacier surge is a sudden speedup of glacier flow coinciding with a large advance of the ice front. Some glaciers surge periodically every 10–100 years, and so surge mechanism is thought to be independent of climate change. However, some recent surges have evacuated so much ice that another surge is unlikely to occur in the same place again. A glacier surge at the Vavilov Ice Cap, Russia, is one of these cases. Since 2013, the glacier has drained more than 11% of the ice basin (9.5 Gt) into the ocean. After the initial surge in 2013, the glacier still retains fast flow at around 1.8 km/year, an unusually high and long-lasting speed for a glacier surge. To understand the future of the surge, we use satellite images to calculate surface elevations and ice speeds, and analyze their change over time for the glacier. The results reveal that the glacier now physically behaves more like an "ice stream," a stream of fast-flowing ice within an ice sheet, which can probably flow at high speed for a long time and drain ice efficiently. This is the first documented case of an ice stream-like feature ever being formed.

1. Introduction

Glacier dynamic instabilities can be triggered in several different ways, such as by changes in basal conditions (Dunse et al., 2015; McMillan et al., 2014; Murray et al., 2002), frontal ice advance or retreat (Nuth et al., 2019; Willis et al., 2018), or loss of buttress support from either an ice shelf or moraine sediment (Benn et al., 2007; De Angelis & Skvarca, 2003; Goldberg, 2017; Willis et al., 2018). A glacier surge, defined as a sudden and short-lived fast glacier acceleration (Clarke et al., 1986; Dowdeswell et al., 1991; Meier & Post, 1969), is a common expression of glacier instability and has been observed in all major glacierized areas of the world except for Antarctica (Sevestre & Benn, 2015). In the traditional sense, a surge-type glacier has a poorly developed hydraulic drainage system, and ice mass builds up over time in the accumulation zone until the glacier reaches a critical driving stress (e.g., Sevestre & Benn, 2015). After this, a surge begins with significant downstream ice transport and frontal advance. A typical surge only lasts for a few months to years (Dowdeswell et al., 1991), after which the glacier returns to its quiescent phase and starts to accumulate ice mass again for 10–100 years (Clarke et al., 1986; Cuffey & Paterson, 2010). This cyclic process is thought to be independent of climate perturbations (Dowdeswell et al., 1991). However, recent surges in Svalbard and the Russian Arctic challenge this hypothesis; these Arctic surges have undergone irreversible ice mass loss in a short period, which is likely triggered by different factors (Dunse et al., 2015; Murray et al., 2012; Nuth et al., 2019; Willis et al., 2018).

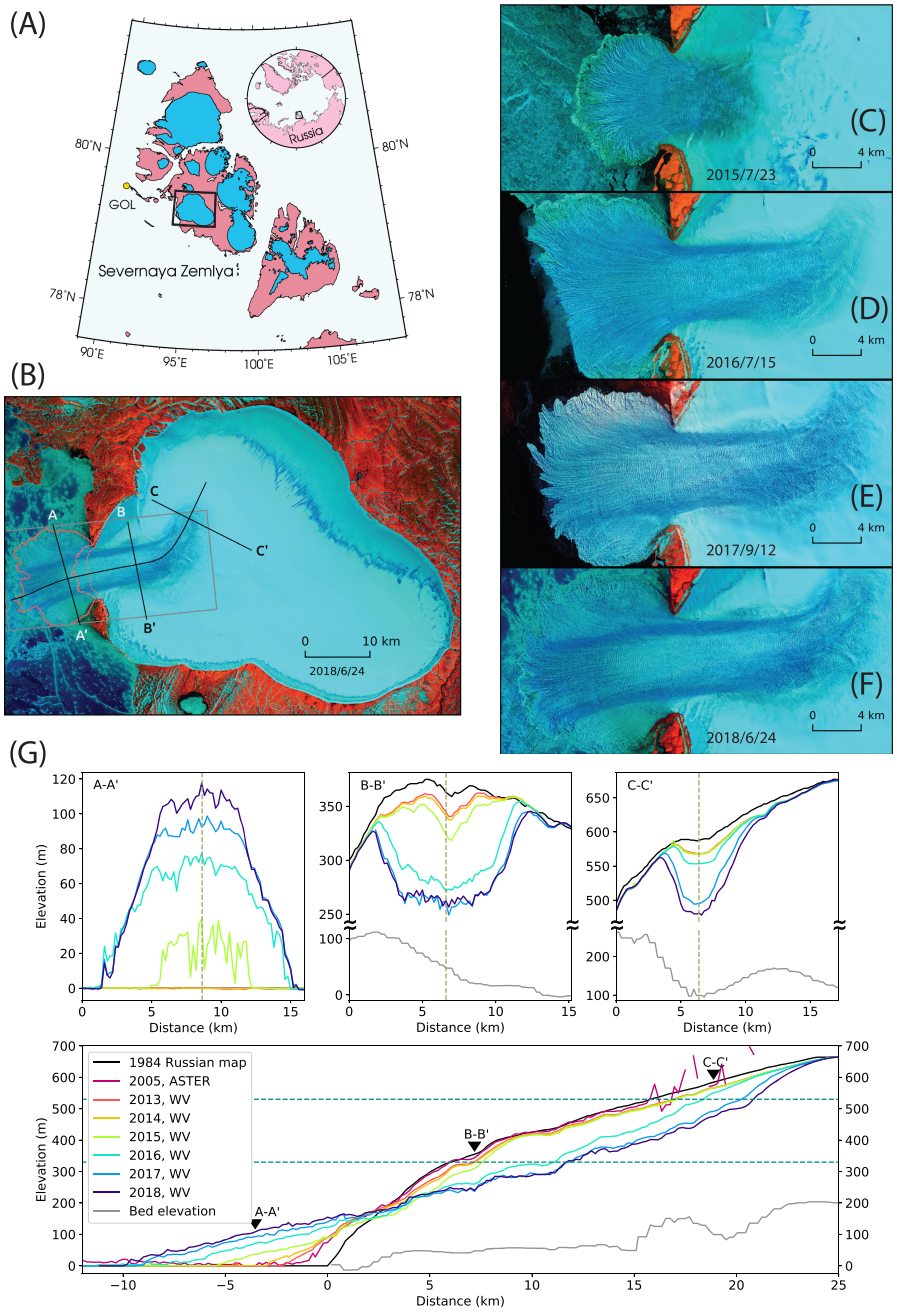

Figure 1. (a) Map of Severnaya Zemlya showing Vavilov Ice Cap (rectangular box) and Golomyanny Island weather station (GOL). Blue ice outlines are from the Randolph Glacier Inventory 6.0. (b) Landsat 8 false-color composite (SWIR-NIR-Blue) from 24 June 2018. Gray box shows the extent of panels (c)–(f). Dotted, dashed, and solid pink lines represent the terminus position in 1984, 2013, and 2016, respectively. Black lines indicate the center flowline and three profiles used in the lower panel. (c–f) Landsat 8 false-color composites with dates shown. Note the propagation of the shear margins (horizontal stripes with darker reflectance) since 2016. (g) Evolution of ice elevation from 1984 to 2018 along three cross-sectional profiles (dubbed A–A′ to C–C′) and the center flowline, with basal topography. Teal dashed lines indicate estimates of equilibrium line altitudes (330–530 m). The intersections of three cross-sectional profiles and the flowline profile are marked as brown dashed lines or black triangles.

Vavilov Ice Cap, Severnaya Zemlya, Russia (79°18′N, 94°40′E), destabilized in 2013 likely due to the loss of frontal support when one of its marine-terminating glaciers advanced and overran weak marine sediment (Willis et al., 2018; Figure 1). The first active stage of the collapse between 2013 and 2016 resembles a typical surge phase due to its significant frontal advance and mass redistribution. During this time, the glacier terminus advanced ~10 km from the precollapse terminus position (Figure 1g) and subsequently formed a mostly grounded piedmont fan (Willis et al., 2018; Figures 1c–1f). Between 2015 and 2016, the glacier speed reached a maximum number of 26 m/day (9.5 km/yr; Bushueva et al., 2018; Willis et al., 2018) with a negative mass balance of −4.5 Gt/yr (0.9% of the mass of the entire ice cap; Willis et al., 2018).

Unlike many other surge-type glaciers, there are no historical records or morainal evidence of a glacier surge at Vavilov (Bushueva et al., 2018; Dowdeswell & Williams, 1997; Willis et al., 2018). The high rate of ice loss at Vavilov makes recovery to presurge conditions unlikely considering the polar desert climate (Moholdt et al., 2012; Willis et al., 2018) and the elevation loss that has moved 14% of the area of the ice cap to below the equilibrium line altitude (ELA). The collapse slowed down in 2016 but did not stop, and is still ongoing in 2019. Elevations along the highly crevassed outlet glacier continue to drop, and ice-thinning area is propagating both upstream and laterally as seen from Figure 1g. The shear margins of the glacier have also expanded from the coastal region of the ice cap into both the interior and the offshore piedmont fan (Figures 1e–1f). The formation of shear margins over the course of 2–3 years has not been observed at any other glaciers, to our knowledge. The outlet has maintained a high flow rate (>1 km/yr) for 6 years, which is longer than a typical Svalbard-type surge that usually lasts 1–5 years (Clarke et al., 1986; Dowdeswell et al., 1991).

The rapid ice flow at Vavilov is not bounded by any bedrock and is only loosely controlled by subglacial topography (Figures 2a–2d and 2i). The extended shear margins that formed since 2016 give the glacier an ice stream-like appearance. An ice stream is usually defined as a grounded area of enhanced ice flow within an ice sheet or an ice cap, bounded laterally by ice and without visible rock boundaries (Cogley et al., 2011; Cuffey & Paterson, 2010; also, see section 4.3). However, whether an outlet glacier can transition to an ice stream remains uncertain. Apart from the well-known shutdown of the Kamb ice stream in Antarctica (Anandakrishnan & Alley, 1997; Catania et al., 2003; Joughin et al., 2002), the evolution of an ice stream, including its formation, has never been recorded. A prolonged ice sheet surge (i.e., a surge that takes place at a sector of an ice sheet rather than an individual outlet glacier) might be a physical cause of ice stream formation (Fowler & Johnson, 1996), but such a surge has never been observed either (De Angelis & Skvarca, 2003; Joughin, Smith, Howat, et al., 2010). Additionally, a glacier surge evacuates its reservoir ice quickly (Clarke et al., 1986; Engelhardt & Kamb, 2013) while an ice stream may maintain a more or less stable mass balance (which can be either positive or negative) for a long time (Cuffey & Paterson, 2010; Rignot & Thomas, 2002; Shepherd et al., 2012). Given the much smaller volume of Vavilov Ice Cap than the Greenland or Antarctic Ice Sheet, it is unclear if the outlet glacier at Vavilov will last long enough to be categorized as an ice stream.

Here we use dense elevation and velocity time series derived from high-resolution satellite optical and synthetic-aperture radar (SAR) images to constrain the physical processes that occur at Vavilov Ice Cap. We aim to better understand the prolonged evolution of the glacier acceleration and thinning and to physically characterize ice flow changes (including a possible transition from a surging glacier to an ice stream). We model the thinning perturbation as a diffusive kinematic wave and calculate the Péclet number (P_e) to determine if the ice flow dissipates a perturbation advectively or diffusively over time (Felikson et al., 2017). Lastly, we compare our time series with local weather data to understand the impact of weather variations on the temporal behavior of the glacier.

2. Data and Methods

We use digital surface models (DSMs) generated from along-track WorldView-1, -2, and -3 satellite optical stereo pairs from 2013–2019. DSMs from 2013–2016 are from the open-access ArcticDEM data set (www.arcticdem.org; Porter et al., 2018), processed using the SETSM (Surface Extraction from TIN-based Searchspace Minimization) software (Noh & Howat, 2015). To extend the time series, we use SETSM to generate additional WorldView-DSMs from 2017–2019. We use ICESat elevation returns over nonglacierized areas as a standard reference to align all DSMs and calculate DSM uncertainty (Text S1 in the supporting information; Melkonian et al., 2016; Zheng et al., 2018). We mosaic DSMs from March to April each year to

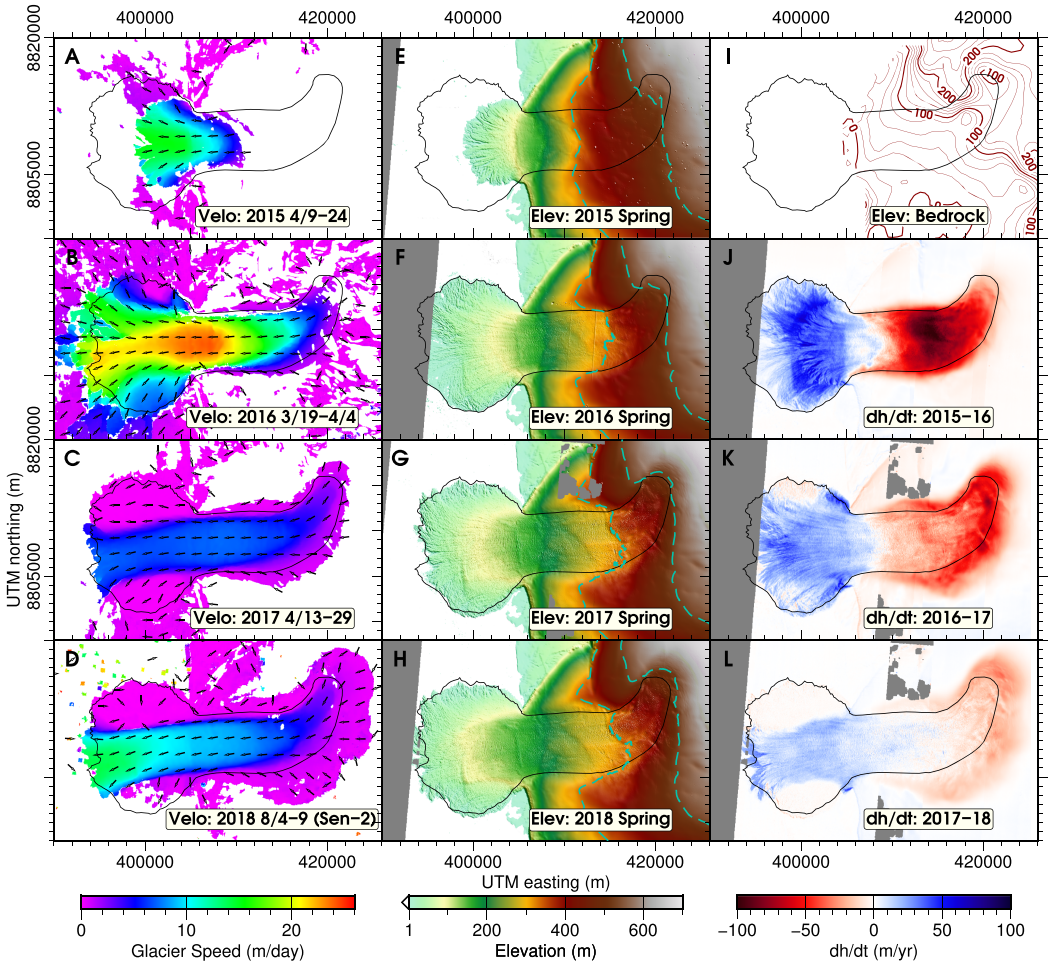

Figure 2. Time series of ice velocity from Landsat 8 (a–c) and Sentinel-2 (d), surface elevation from WorldView DEMs (e–h), basal elevation from airborne radar sounding (i) (Bassford et al., 2006; Dowdeswell et al., 2002), and elevation difference (j–l). The black outline in all panels shows the extent of the collapse in the 2016 spring. Teal dashed lines in panels (e)–(h) indicate the boundary of ELA (see Figure 1).

produce elevation maps and calculate annual elevation change. In order to estimate the ELA, we identify the snow line location from Landsat 8 late-summer images around the entire ice cap and read the corresponding elevations from the DSMs. The annual ice volume change and annual ice mass change above sea level are derived from the elevation change, assuming a fixed ice density of 850 ± 60 kg/m^3 (2 sigma; Huss, 2013; Zheng et al., 2018). We also estimate the total ice mass of the collapsed basin using the glacier outline from Randolf Glacier Inventory version-6 (Pfeffer et al., 2014) and the density assumed here. Other elevation products used include a digitized cartographic map from 1984 and an ASTER DSM from 2005 as reference elevations before the collapse (Figure 1g; Willis et al., 2018). We also use bedrock depths from an airborne radar sounding survey in 2007 (Bassford et al., 2006; Willis et al., 2018; Figure 2i) to calculate ice thickness. Table S1 provides a complete list and the details of all elevation products we use in this study, and Text S1 provides an overview of the quality of each data set.

Glacier velocities from 2013–2019 are obtained through pixel tracking (e.g., Fahnestock et al., 2016; Joughin, Smith, & Abdalati, 2010; Kääb et al., 2016; Paul et al., 2015; Strozzi et al., 2002) on pairs of optical (Landsat 8 and Sentinel-2) and SAR (Sentinel-1, Radarsat-2, and ALOS-2) images. We utilize the workflow described in Willis et al. (2018) with minor changes described in Text S2. We developed an open-source software package called "Cryosphere And Remote Sensing Toolkit (CARST)" (https://github.com/whyjz/CARST; Zheng et al., 2019) in order to access modules from GDAL and the InSAR Scientific Computing Environment (Rosen et al., 2004). These modules are integrated into a simple workflow in CARST. Besides, velocities from Radarsat-2 (2016–2017), Sentinel-1 (2016–2019), and ALOS-2 PALSAR-2 (2015–2016) were computed using

all available data by Strozzi et al. (2017) and have been shared with us. Table S2 provides a complete list of the satellite image pairs we use in this study.

The closest weather station to Vavilov Ice Cap is on Golomyanny Island (79°33′N, 90°37′E, Figure 1), ~80 km NW of the outlet glacier. Weather station data are available online (https://rp5.ru/Weather_archive_on_Golomyanny_Island since 2005 and https://climexp.knmi.nl since 1936; see Text S3 for details), and in this study we use all the available records from 1936 to 2019. The positive degree day sum (PDD; Text S3) is used as a proxy for summer melt (e.g., Barrand et al., 2013; Nuth et al., 2019).

We use the force budget method described in Van Der Veen and Whillans (1989) to calculate the driving stress and three balancing resistive stresses: basal drag, longitudinal stress gradients, and lateral drag, assuming the acceleration of the ice flow is negligible at any given time. Details are described in Willis et al. (2018).

To determine if the ice flow responds to perturbations advectively or diffusively, we use the Péclet number (P_e) and assume a hard-bed sliding law (Weertman, 1957). Following the equations set up by Nye (1963); Bindschadler (1997); Felikson et al. (2017) with the input of the observed glacier velocity, P_e can be expressed as

$$P_e = \left[\frac{(m+1)\alpha}{mH} - \frac{U'}{U} - \frac{H'}{H} + \frac{\alpha'}{\alpha}\right] l, \quad (1)$$

where m is the flow law parameter, U is ice speed along a flowline, H is ice thickness, α is surface slope, and l is characteristic length. U, H, and α are sampled from observations and vary with distance away from the ice divide, and $U^{'}$, $H^{'}$, and $\alpha^{'}$ are their first-order derivative with respect to the distance. The parameter m is set to 3 in this study. Changing m does not significantly affect P_e since m only exists in the first term of the equation as a form of $\frac{m+1}{m}$, which roughly equals to 1. Detailed steps in deriving this equation are provided in Text S4. A highly advective alpine valley glacier with a constant speed, a constant surface slope of 10°, and a constant ice thickness of 200 m yields a Péclet number around 10; an outlet glacier in the Greenland ice sheet typically has a value below 3 except for some areas with steep bed topography (Felikson et al., 2017). On the other hand, a typical Siple Coast ice steam (slope = 0.0012, thickness = 1,000 m, Perol et al. 2015) has a P_e of ~0.02 (Bindschadler, 1997) assuming a constant glacier speed. Here we set l at 10,000 m, which represents the approximate length of the thinning perturbation along the flowline (e.g., Figure 2j).

3. Results

3.1. Elevation Change

The destabilization began in 2013 at a lower altitude, 0–100 m below the lowest estimate of the ELA (330 m), and slowly migrated inland. During 2015–2016 the glacier reached the maximum thinning rate at ~100 m/yr (Figure 2j; Willis et al., 2018) in the region of the ELA (330–530 m). The geodetic mass balance between 2013 and 2019 is −9.49 ± 0.69 Gt (2 sigma interval), which accounts for 11% of the ice mass of the entire basin (~84 Gt). The annual mass balance data are available in Table S3.

The centroid of thinning continued to move upstream after the main collapse (Figures 2j, 2k, and 4d). In 2017–2018, it went past the highest estimate of the ELA. Rapid thinning of about 10 m/yr is observed almost to the ice divide (the 25 km mark on Figure 1g) in 2018. The upstream section of the thinning glacier lies roughly within a bedrock channel (Figure 2i), which may explain the curvature of the ice flow due to greater ice thickness and driving stresses.

Since 2016 the terminus began to fluctuate in a position by about 2 km (Figures 2f–2h). The terminus may have temporarily achieved flotation when it stopped advancing (Figure 1g; Willis et al., 2018); however, the height at the front of the piedmont fan grows over time after 2016 within ±4 km from the center flowline (Figures 1A–A′ and 1g; Figures 2h and 2l), suggesting that it is grounded more recently. Furthermore, after 2016 the north and south flanks of the piedmont fan stagnated, suggesting that they are grounded as well.

3.2. Glacier Velocity and Its Correlation With Temperature

The velocities between 2015 and 2019 from different data sets and sources (Figure 3b) highly agree with each other within their 95% confidence interval (e.g., Figure S2). The mean uncertainty (1 sigma) of Landsat 8, Sentinel-2, and Sentinel-1 velocities processed with CARST is 0.34 m/day, 0.22 m/day, and 0.78 m/day, respectively. RADARSAT-2 velocity is estimated to have an uncertainty of 0.014 m/day (5 m/yr; Strozzi et al., 2017). The uncertainty of the Sentinel-1 velocities from Strozzi et al. (2017) is 0.17 m/day (63 m/yr) based

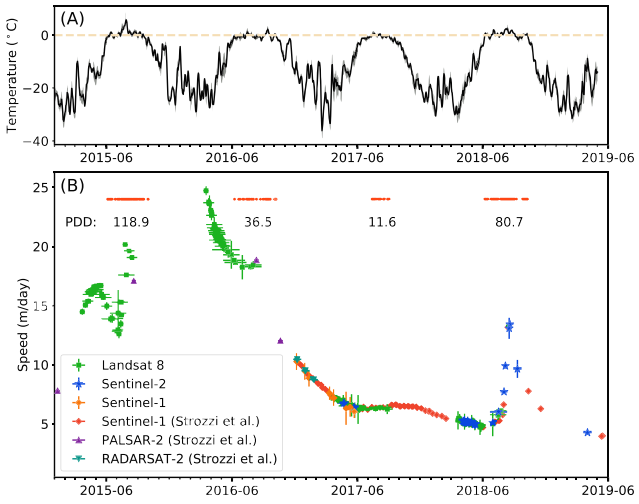

Figure 3. (a) Five-day running mean of the daily mean temperature from Golomyanny Island in 2015–2019, bounded by the daily minimum and maximum temperature gray-shaded area. (b) Glacier speed at the centerline of the 1984 terminus position at the same time, measured from several optical and SAR sensors (see legend). Each point is an average speed during the period bounded by its horizontal bar, with the 2 σ uncertainty indicated by the vertical bar. Small red dots in the upper part of the plot are days with a positive daily mean temperature, and the associated numbers are the positive degree day sum (PDD) for each year.

on the standard deviation of the difference between Sentinel-1 and RADARSAT-2 velocity. From the glacier velocity at the trunk of the channel (Figure 3b), at least one slowdown and speedup event have been identified during summer 2015: the glacier speed dropped to 12 m/day in July but quickly went even higher than before to 20 m/day in August. The speed reached a maximum of 25 m/day in the subsequent winter and began to slow down gradually for 2 years. During July and August 2018, the glacier speed suddenly increased almost threefold, from 5 m/day to ∼14 m/day. This acceleration and speed up only lasted for about 3 months, with speeds returning to 5 m/day the following winter.

The pattern of glacier speed has also evolved (Figures 2a–2d, S3, and Movie S1). In 2016/2017, the maximum speed appears at the boundary of reservoir/receiving zone near the ELA, which is typical for a glacier surge (Fu et al., 2019; Nuth et al., 2019; Wendt et al., 2017). However, during the 2018 speedup event the maximum speed is observed near the terminus. We observe ice mass spreading out to form a piedmont fan between 2013 and 2016 (Figures 2a and 2b), but subsequently in 2017, the flanks of the fan become stagnant since its velocity dropped to nearly zero (Figures 2c and 2d). At the boundary of the new fast-flowing channel, we observe more marginal crevasses from Figures 1e and 1f, which is interpreted as the formation of shear margins. The area of the new channel also corresponds to the area of thickening after 2017 (Figure 2l).

Both the 2015 and 2018 summer speedups correspond to the timing of positive degree days (Figure 3). The glacier speed started to increase when the summer temperature in Golomyanny Island stayed above the freezing point for about 1–2 months. Additionally, both 2015 and 2018 have a higher PDD than years with a weak or no summer speedup (2016 and 2017). If compared to the long-term average (1936–2018, see Table S4), these two years are 30–100% higher than the average (PDD ≈ 60).

3.3. Variation in Force Balance and Reaction to Perturbation Over Time

Willis et al. (2018) noted that the basal drag significantly reduced in 2016 compared to 2013. The force balance results (Figures 4a–4c) indicate that the trend continued to 2017, with the basal drag eventually dropping to around zero in the spring of 2018. At that time the driving stresses are nearly fully balanced by the longitudinal stress gradients and lateral drag. The shear margins, including the part in the piedmont fan, seem to stabilize by spring 2017 because subsequent changes to the lateral drag are small. There is an area in the upper, easternmost part of the glacier where lateral drag points in a different direction, suggesting a new branch of glacier channel forming to the south of the main channel.

Figure 4d shows the Péclet number along the center flowline over time between 2014 and 2018. A small $|P_e|$ means that any perturbations within the ice flow is dominated by diffusion, a typical mode in an ice stream (Bindschadler, 1997). Figure 4e plots the advective strength (speed) versus the diffusivity along the flowline for each year. Note that P_e can be positive or negative, meaning that the kinematic wave can propagate either downstream or upstream. The advective speed corresponds to the migration rate of the thinning center. For example, in 2015 the ice flow near the thinning center (red circle in Figures 4d and 4e) has an advective speed of −9 m/day, and in 2016 the advective speed near the thinning center decreases to −25 m/day (yellow circle in Figures 4d and 4e. The average of the two advective speeds is close to the rate of the thinning center migration between 2014 and 2016 (−17.7 m/day or −6.46 km/yr, see Figure S1).

The years 2015 and 2016 show a relatively strong influence ($|P_e| > 3$) of advection somewhere along the profile, although the location has changed and migrated upstream. Starting from 2017, P_e became low everywhere along the profile ($|P_e| < 1.8$). Figure 4e indicates that this is likely due to a change to a larger diffusivity in larger area caused by the flattening of the surface. Since 2016, the entire lower portion of the flowline profile (0–13 km from the 1984 terminus) shows a diffusivity around or more than 2×10^5 m^2/day, a value more similar to a typical ice stream (2×10^6 m^2/day) than a normal glacier (3×10^3 m^2/day; Bindschadler, 1997).

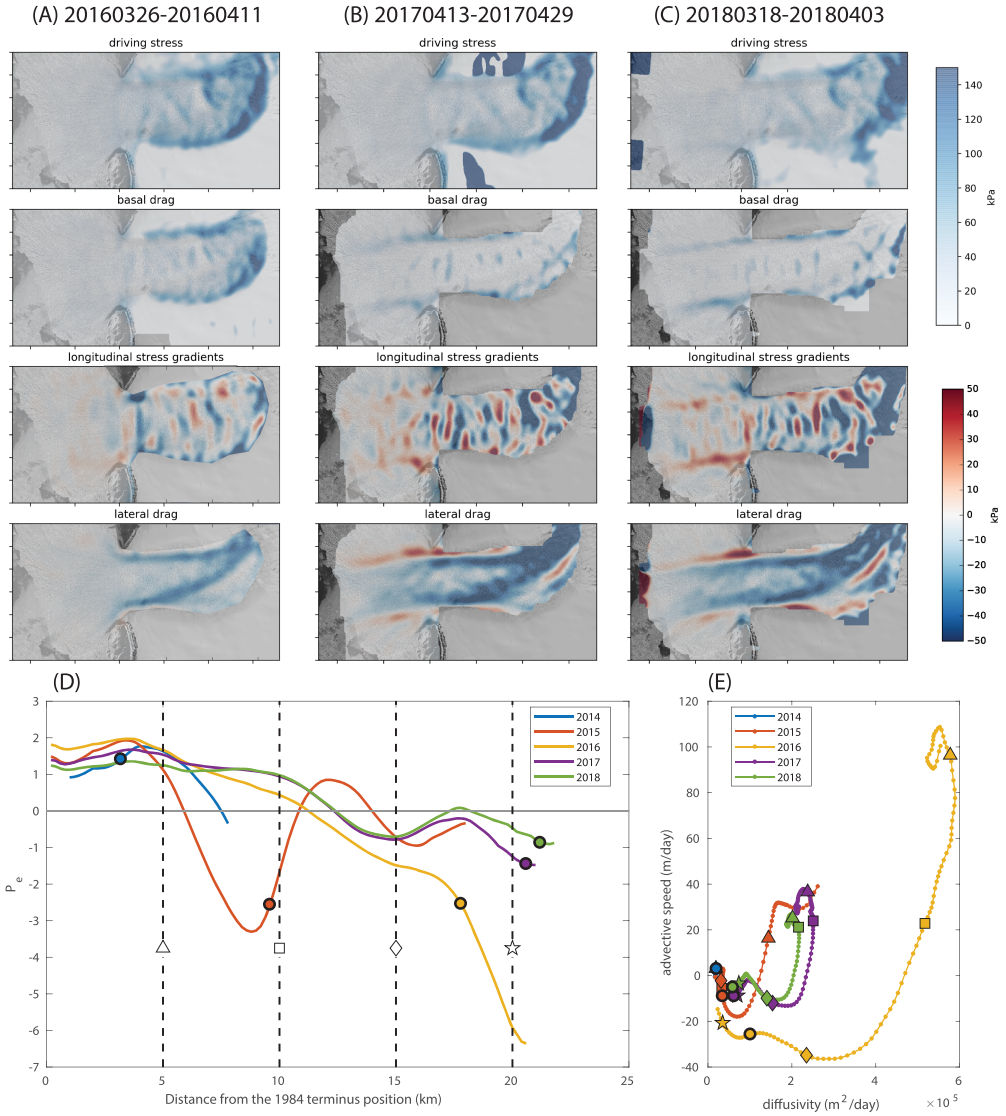

Figure 4. (A–C) Spring glacier force balance results in 2016–2018. Note the sudden decrease in basal drag after 2016 and the increase of lateral drag over time. (D) Péclet number (P_e) along the flowline during 2014–2018. Every 5 km is marked with a distinct symbol, and the thinning center location for each year is marked with a circle. (E) The advective speed ($c_0 - \frac{\partial D_0}{\partial x}$) versus the diffusivity (D_0) from each year. Marked places on each line correspond to the specified mark locations from panel D, and smaller dots are plotted every 200 m along the flowline.

4. Discussion

4.1. Summer Speedup Events

Many tidewater glaciers and ice streams show periodic summer speedups (e.g., Dunse et al., 2015; Kehrl et al., 2017; Neckel et al., 2016; Schellenberger et al., 2017; Sevestre et al., 2018). This is due to seasonal variation in subglacial hydrology that greatly affects the glacier sliding speeds (Sevestre et al., 2018). During summer, melt can penetrate to a glacier bed and lubricate the interface, causing higher glacier speeds (Dunse et al., 2015). The summer speedup in 2018 seems to fit this pattern, as the highly crevassed glacier channel provides an easy way for surface melt to percolate down to the bed (e.g., Dunse et al., 2015; Gong et al., 2018). Moreover, the speed pattern of 2015 (Figure 3) resembles one of the seasonal velocity modes of Greenland glaciers (Moon et al., 2014). When surface meltwater is drained quickly to the bed in the summer, channels at the bed efficiently transport water to the coast. The effective water pressure thus drops, slowing down the glacier. When part of the subglacial channels begins to refreeze during early fall and the channels narrow, effective water pressure increases due to an increasingly inefficient drainage system, speeding up the glacier (Moon et al., 2014). However, the speedup at Vavilov occurred in August 2015 when monthly temperature

was the highest during the year (Figure 3) instead of early fall, which might indicate other factors affecting the pattern, such as the relationship between terminus advance and glacier slowdown (Moon et al., 2014). Nevertheless, the sustained warmer summer air temperature in both 2015 and 2018 (Figure 3) still provides a potential link of the seasonal speedups with the supply of surface melt.

Whether there was a late summer speedup in 2016 remains somewhat ambiguous due to a data gap. During June–August 2016 and July–September 2017, the glacier speed roughly stayed the same. This might suggest that a small speedup component canceled out the decreasing trend of the ice speed, and a colder-than-usual summer weather in both years (only half of the long-term PDD) might explain this smaller anomaly.

4.2. Formation of the Shear Margins in the Piedmont Fan

To our knowledge, this is the first time that the formation of shear margins within an offshore piedmont fan has been observed. Typically, shear margins form due to a transition in ice thickness (Rippin et al., 2004), basal strength (Anandakrishnan et al., 1998; Rippin et al., 2004), thermal regime (Jacobson & Raymond, 1998), or subglacial hydrology (Bougamont et al., 2011; Tulaczyk et al., 2000) across the margin. Since the piedmont fan lies on the seafloor, there is likely minimal cross-flow variability in ice thickness or basal conditions. We thus propose an alternative mechanism here: the new shear margins formed when the entire piedmont fan stagnated in the 2016/2017 winter. During this time, the glacier was still flowing fast (~1.6 km/yr), advecting a substantial volume of ice downflow. Driving stresses over the flat piedmont were low, as were basal drag (over weak marine sediments) and longitudinal stress gradients (Figure 4). Driving stress, while small, was still larger in the along-flow direction than across-flow. Thus, while small amounts of ice continued to flow laterally, thickening the flanks of the piedmont (Figure 2k), the constant advection of fast-moving ice within the laterally confined trunk damaged the piedmont flanks, creating distinct shear margins. Once the shear margins formed, they stabilized the new channel by providing support from the stagnant ice adjacent to the channel.

4.3. Transition From a Collapse to an Ice Stream

There is a wide range of ice stream properties, but typically an ice stream has a gentle and uniform slope throughout its highly crevassed channel that is bounded by shear margins (Cogley et al., 2011; Truffer & Echelmeyer, 2003). Shear margins typically restrict the width of an ice stream. Some ice streams are only a few kilometers wide, while others are tens of kilometers in width. Ice stream speeds are typically from 50 m/yr to 1 km/yr, while ice speeds adjacent to the ice stream are much lower, only a few meters per year (Joughin et al., 2002).

During the collapse of the Vavilov Ice Cap, a new outlet glacier formed with an ice stream-like geometry and velocity pattern. When the major collapse initiated in 2014/2015, diffusivity was low (mostly $< 1\times10^5$ m^2/day, Figure 4e) and the perturbation at the thinning center (8–10 km distance from 1984 terminus) was dominated by advection. The negative P_e (~ -3, Figure 4d) suggests that the thinning perturbation was propagating upstream. In 2016, the downstream region (0–15 km distance from 1984 terminus) reached a high diffusivity ($> 2\times10^5$ m^2/day) and a low $|P_e|$ while the upstream region still underwent advection ($P_e \approx -6$). In 2017/2018, $|P_e|$ decreased along the entire ice stream, even at the upstream area. This suggests the collapse entered a new regime in 2017 when perturbations in ice thickness began to evolve more diffusively, like an ice stream rather than a glacial collapse. From this study, we suggest that the threshold between the normal glacier flow during the collapse and formation of ice stream-like flow may be defined as $|P_e| < 2$ or diffusivity $> 1.5\times10^5$ m^2/day.

The analysis of P_e also shows that once a glacier begins to collapse, P_e is likely to decrease, causing thinning or thickening perturbations to diffuse inland (or advect inland if P_e is negative enough). A similar process has been observed in many tidewater glaciers of Svalbard (e.g., McMillan et al., 2014; Murray et al., 2012; Nuth et al., 2019; Sevestre et al., 2018; Strozzi et al., 2017). Fowler and Johnson (1996) point out mathematically that this process can also take place on an ice sheet and subsequently form an ice stream, although an ice sheet surge has never been observed in the modern data records. The destabilization of Vavilov Ice Cap provides an analogy for the formation of an ice stream at larger ice sheets, as the major cause of the destabilization is due to the reduction of basal drag when the glacier advanced on to weak marine sediment (Willis et al., 2018). As marine ice sheets are eroded by warm marine water, they are likely to be subjected to instability due to the removal of buttressing ice shelves (Goldberg, 2017; Pollard et al., 2015). Once debuttressing has occurred, ice streams may form, which can efficiently evacuate ice into the global ocean within a surprisingly short time.

5. Conclusions

We document the evolution of surface elevation, velocity, and mass balance between 2013 and 2019 on the destabilized Vavilov Ice Cap. We identify a summer speedup event from both 2015 and 2018 that correlates to a sustained warm summer. New shear margins appeared in the piedmont fan in 2017, coincident with the pattern shifts of both glacier velocity and elevation change. The evidence indicates that the ice dynamics have entered a new regime that is similar to ice streams. A transition of response behavior is recognized using Péclet number, which suggests advection-dominated ice mass wasting before 2016 and diffusion-dominated ice mass transport after 2017. The analysis using Péclet number explains the natural migration of the thinning center and provides us a threshold to identify the ice-stream formation after 2017. Since the mechanism of the collapse is similar to a removal of ice shelves in front of a marine ice sheet, the formation of ice stream at the boundaries of a marine ice sheet is anticipated in the future under plausible global warming scenarios.

Acknowledgments
WorldView imagery (including the ArcticDEM dataset) was created from DigitalGlobe, Inc., and was provided by the Polar Geospatial Center at the University of Minnesota, which is supported by NSF Grants 1043681, 1559691, and 1542736. This work utilized the RMACC Summit supercomputer, which is supported by the National Science Foundation (Awards ACI-1532235 and ACI-1532236), the University of Colorado Boulder, and Colorado State University. The Summit supercomputer is a joint effort of the University of Colorado Boulder and Colorado State University. Sentinel data are found through The Copernicus Open Access Hub (https://scihub.copernicus.eu). Landsat and Sentinel-2 data are downloaded via the USGS Earth Explorer (https://earthexplorer.usgs.gov), and Sentinel-1 data are downloaded via Alaska Satellite Facility's Data Search portal (https://search.asf.alaska.edu). The Randolph Glacier Inventory version-6 data can be found at https://www.glims.org/RGI/. Acquisition of airborne radar data on bed elevations was funded by UK NERC Grant GR3/9958 and can be found at https://doi.org/10.5281/zenodo.3478524 with additional restrictions (see the associated Data Availability Statement). ICESat data (GLAH06 data set available at https://nsidc.org/data/icesat/data.html) were generously processed and provided by Geir Moholdt of the Norwegian Polar Institute. We thank Tazio Strozzi and the ESA Glaciers CCI project (www.esa-glaciers-cci.org) for providing glacier velocities from Radarsat-2, ALOS-2, and Sentinel-1. The derived glacier velocity product using CARST and the additional elevation data are available at https://doi.org/10.5281/zenodo.3478524. Whyjay Zheng acknowledges the support from the Overseas Ph.D. Scholarship granted by the Ministry of Education, Taiwan. We thank Jenny Suckale and Paul Summers for helpful discussions. We also thank Denis Felikson and an anonymous reviewer for their invaluable comments on improving the quality of this paper.

References

Anandakrishnan, S., & Alley, R. B. (1997). Stagnation of ice stream C, West Antarctica by water piracy. *Geophysical Research Letters*, *24*(3), 265–268. https://doi.org/10.1029/96GL04016

Anandakrishnan, S., Blankenship, D. D., Alley, R. B., & Stoffa, P. L. (1998). Influence of subglacial geology on the position of a West Antarctic ice stream from seismic observations. *Nature*, *394*(6688), 62–65. https://doi.org/10.1038/27889

Barrand, N. E., Vaughan, D. G., Steiner, N., Tedesco, M., Kuipers Munneke, P., Van Den Broeke, M. R., & Hosking, J. S. (2013). Trends in Antarctic Peninsula surface melting conditions from observations and regional climate modeling. *Journal of Geophysical Research: Earth Surface*, *118*, 315–330. https://doi.org/10.1029/2012JF002559

Bassford, R. P. P., Siegert, M. J., & Dowdeswell, J. A. (2006). Quantifying the mass balance of ice caps on Severnaya Zemlya, Russian High Arctic II: Modeling the Flow of the Vavilov Ice Cap under the Present Climate. *Arctic, Antarctic, and Alpine Research*, *38*(1), 13–20.

Benn, D. I., Warren, C. R., & Mottram, R. H. (2007). Calving processes and the dynamics of calving glaciers. *Earth-Science Reviews*, *82*(3-4), 143–179. https://doi.org/10.1016/j.earscirev.2007.02.002

Bindschadler, R. (1997). Actively surging West Antarctic ice streams and their response characteristics. *Annals of Glaciology*, *24*, 409–414. https://doi.org/10.3189/S0260305500012520

Bougamont, M., Price, S., Christoffersen, P., & Payne, A. J. (2011). Dynamic patterns of ice stream flow in a 3-D higher-order ice sheet model with plastic bed and simplified hydrology. *Journal of Geophysical Research*, *116*, F04018. https://doi.org/10.1029/2011JF002025

Bushueva, I. S., Glazovsky, A. F., & Nosenko, G. A. (2018). Surge development in the western sector of the Vavilov Ice Cap, Severnaya Zemlya, 1963–2017 (in Russian). *Lod i Sneg (Ice and Snow)*, *58*(3), 293–306. https://doi.org/10.15356/2076-6734-2018-3-293-306

Catania, G. A., Conway, H. B., Gades, A. M., Raymond, C. F., & Engelhardt, H. (2003). Bed reflectivity beneath inactive ice streams in West Antarctica. *Annals of Glaciology*, *36*, 287–291. https://doi.org/10.3189/172756403781816310

Clarke, G. K. C., Schmok, J. P., Ommanney, C. S. L., & Collins, S. G. (1986). Characteristics of surge-type glaciers. *Journal of Geophysical Research*, *91*(5), 7165–7180. https://doi.org/10.1029/JB091iB07p07165

Cogley, J. G., Hock, R., Rasmussen, L. A., Arendt, A. A., Bauder, A., Braithwaite, R. J., et al. (2011). *Glossary of glacier mass balance and related terms*. IHP-VII Technical Documents in Hydrology No. 86, IACS Contribution No. 2, UNESCO-IHP, Paris. https://doi.org/10.1657/1938-4246-44.2.256b

Cuffey, K., & Paterson, W. S. B. (2010). *The physics of glaciers* (4th ed.). Amsterdam: Elsevier Inc.

De Angelis, H., & Skvarca, P. (2003). Glacier surge after ice shelf collapse. *Science*, *299*(5612), 1560–1562. https://doi.org/10.1126/science.1077987

Dowdeswell, J. A., Bassford, R. P., Gorman, M. R., Williams, M., Glazovsky, A. F., Macheret, Y. Y., et al. (2002). Form and flow of the Academy of Sciences Ice Cap, Severnaya Zemlya, Russian High Arctic. *Journal of Geophysical Research*, *107*(B4), EPM 5–1–EPM 5–15. https://doi.org/10.1029/2000JB000129

Dowdeswell, J. A., Hamilton, G. S., & Hagen, J. O. (1991). The duration of the active phase on surge-type glaciers: Contrasts between Svalbard and other regions. *Journal of Glaciology*, *37*(127), 388–400. https://doi.org/10.3189/S0022143000005827

Dowdeswell, J. A., & Williams, M. (1997). Surge-type glaciers in the Russian High Arctic identified from digital satellite imagery. *Journal of Glaciology*, *43*(145), 489–494. https://doi.org/10.3189/S0022143000035097

Dunse, T., Schellenberger, T., Hagen, J. O., Kääb, A., Schuler, T. V., & Reijmer, C. H. (2015). Glacier-surge mechanisms promoted by a hydro-thermodynamic feedback to summer melt. *Cryosphere*, *9*(1), 197–215. https://doi.org/10.5194/tc-9-197-2015

Engelhardt, H., & Kamb, B. (2013). Kamb ice stream flow history and surge potential. *Annals of Glaciology*, *54*(63), 287–298. https://doi.org/10.3189/2013AoG63A535

Fahnestock, M., Scambos, T., Moon, T., Gardner, A., Haran, T., & Klinger, M. (2016). Rapid large-area mapping of ice flow using Landsat 8. *Remote Sensing of Environment*, *185*, 84–94. https://doi.org/10.1016/j.rse.2015.11.023

Felikson, D., Bartholomaus, T. C., Catania, G. A., Korsgaard, N. J., Kjær, K. H., Morlighem, M., et al. (2017). Inland thinning on the Greenland ice sheet controlled by outlet glacier geometry. *Nature Geoscience*, *10*(5), 366–369. https://doi.org/10.1038/ngeo2934

Fowler, A. C., & Johnson, C. (1996). Ice-sheet surging and ice-stream formation. *Annals of Glaciology*, *23*, 68–73. https://doi.org/10.3189/S0260305500013276

Fu, X., Li, Z., & Zhou, J. (2019). Characterizing the surge behavior of Alakesayi Glacier in the West Kunlun Shan, Northwestern Tibetan Plateau, from remote-sensing data between 2013 and 2018. *Journal of Glaciology*, *65*(249), 168–172. https://doi.org/10.1017/jog.2019.2

Goldberg, D. N. (2017). Ice shelf buttressing. *International Encyclopedia of Geography: People, the Earth, Environment and Technology*. https://doi.org/10.1002/9781118786352.wbieg0567

Gong, Y., Zwinger, T., Åström, J., Altena, B., Schellenberger, T., Gladstone, R., & Moore, J. C. (2018). Simulating the roles of crevasse routing of surface water and basal friction on the surge evolution of Basin 3, Austfonna ice cap. *Cryosphere*, *12*(5), 1563–1577. https://doi.org/10.5194/tc-12-1563-2018

Huss, M. (2013). Density assumptions for converting geodetic glacier volume change to mass change. *The Cryosphere*, *7*, 877–887. https://doi.org/10.5194/tcd-7-219-2013

Jacobson, H. P., & Raymond, C. F. (1998). Thermal effects on the location of ice stream margins. *Journal of Geophysical Research*, *103*(B6), 12,111–12,122. https://doi.org/10.1029/98JB00574

Joughin, I., Smith, B. E., & Abdalati, W. (2010). Glaciological advances made with interferometric synthetic aperture radar. *Journal of Glaciology*, *56*(200), 1026–1042. https://doi.org/10.3189/002214311796406158

Joughin, I., Smith, B. E., Howat, I. M., Scambos, T., & Moon, T. (2010). Greenland flow variability from ice-sheet-wide velocity mapping. *Journal of Glaciology*, *56*(197), 415–430. https://doi.org/10.3189/002214310792447734

Joughin, I., Tulaczyk, S., Bindschadler, R., & Price, S. F. (2002). Changes in west Antarctic ice stream velocities: Observation and analysis. *Journal of Geophysical Research*, *107*(B11), EPM 3–1–EPM 3–22. https://doi.org/10.1029/2001JB001029

Kääb, A., Winsvold, S., Altena, B., Nuth, C., Nagler, T., & Wuite, J. (2016). Glacier remote sensing using Sentinel-2. Part I: Radiometric and geometric performance, and application to ice velocity. *Remote Sensing*, *8*(7), 598. https://doi.org/10.3390/rs8070598

Kehrl, L. M., Joughin, I., Shean, D. E., Floricioiu, D., & Krieger, L. (2017). Seasonal and interannual variabilities in terminus position, glacier velocity, and surface elevation at Helheim and Kangerlussuaq Glaciers from 2008 to 2016. *Journal of Geophysical Research: Earth Surface*, *122*, 1635–1652. https://doi.org/10.1002/2016JF004133

McMillan, M., Shepherd, A., Gourmelen, N., Dehecq, A., Leeson, A., Ridout, A., et al. (2014). Rapid dynamic activation of a marine-based Arctic ice cap. *Geophysical Research Letters*, *41*, 8902–8909. https://doi.org/10.1002/2014GL062255

Meier, M. F., & Post, A. (1969). What are glacier surges? *Canadian Journal of Earth Sciences*, *6*(4), 807–817. https://doi.org/10.1038/2031227a0

Melkonian, A. K., Willis, M. J., Pritchard, M. E., & Stewart, A. J. (2016). Recent changes in glacier velocities and thinning at Novaya Zemlya. *Remote Sensing of Environment*, *174*, 244–257. https://doi.org/10.1016/j.rse.2015.11.001

Moholdt, G., Wouters, B., & Gardner, A. S. (2012). Recent mass changes of glaciers in the Russian High Arctic. *Geophysical Research Letters*, *39*, L10502. https://doi.org/10.1029/2012GL051466

Moon, T., Joughin, I., Smith, B., van den Broeke, M. R., van de Berg, W. J., Noël, B., & Usher, M. (2014). Distinct patterns of seasonal Greenland glacier velocity. *Geophysical Research Letters*, *41*, 7209–7216. https://doi.org/10.1002/2014GL061836

Murray, T., James, T. D., Macheret, Y., Lavrentiev, I., Glazovsky, A., & Sykes, H. (2012). Geometric changes in a tidewater glacier in Svalbard during its surge cycle. *Arctic, Antarctic, and Alpine Research*, *44*(3), 359–367. https://doi.org/10.1657/1938-4246-44.3.359

Murray, T., Strozzi, T., Luckman, A., Pritchard, H., & Jiskoot, H. (2002). Ice dynamics during a surge of Sortebræ, East Greenland. *Annals of Glaciology*, *34*(1), 323–329. https://doi.org/10.3189/172756402781817491

Neckel, N., Helm, V., Humbert, A., Rosenau, R., & Ebermann, B. (2016). *Near real time surface velocity measurements of North-East Greenland Ice Stream outlet glaciers from Sentinel-1A data*. Paper presented at ESA Living Planet Symposium, Prague, Czech Republic, 9–13 May 2016.

Noh, M. J., & Howat, I. M. (2015). Automated stereo-photogrammetric DEM generation at high latitudes: Surface Extraction with TIN-based Search-space Minimization (SETSM) validation and demonstration over glaciated regions. *GIScience & Remote Sensing*, *52*(2), 198–217. https://doi.org/10.1080/15481603.2015.1008621

Nuth, C., Gilbert, A., Köhler, A., McNabb, R., Schellenberger, T., Sevestre, H., et al. (2019). Dynamic vulnerability revealed in the collapse of an Arctic tidewater glacier. *Scientific Reports*, *9*(1), 5541. https://doi.org/10.1038/s41598-019-41117-0

Nye, J. F. (1963). The response of a glacier to changes in the rate of nourishment and wastage. *Proceedings of the Royal Society of London. Series A. Mathematical and Physical Sciences*, *275*(1360), 87–112. https://doi.org/10.1098/rspa.1963.0157

Paul, F., Bolch, T., Kääb, A., Nagler, T., Nuth, C., Scharrer, K., et al. (2015). The glaciers climate change initiative: Methods for creating glacier area, elevation change and velocity products. *Remote Sensing of Environment*, *162*, 408–426. https://doi.org/10.1016/j.rse.2013.07.043

Perol, T., Rice, J. R., Platt, J. D., & Suckale, J. (2015). Subglacial hydrology and ice stream margin locations. *Journal of Geophysical Research: Earth Surface*, *120*, 1352–1368. https://doi.org/10.1002/2015JF003542

Pfeffer, W. T., Arendt, A. A., Bliss, A., Bolch, T., Cogley, J. G., Gardner, A. S., et al. (2014). The Randolph glacier inventory: A globally complete inventory of glaciers. *Journal of Glaciology*, *60*(221), 537–552. https://doi.org/10.3189/2014JoG13J176

Pollard, D., DeConto, R. M., & Alley, R. B. (2015). Potential Antarctic Ice Sheet retreat driven by hydrofracturing and ice cliff failure. *Earth and Planetary Science Letters*, *412*, 112–121. https://doi.org/10.1016/j.epsl.2014.12.035

Porter, C., Morin, P., Howat, I., Noh, M.-J., Bates, B., Peterman, K., et al. (2018). ArcticDEM. Harvard Dataverse. https://doi.org/10.7910/DVN/OHHUKH

Rignot, E., & Thomas, R. H. (2002). Mass balance of polar ice sheets. *Science*, *297*(5586), 1502–1506. https://doi.org/10.1126/science.1073888

Rippin, D. M., Bamber, J. L., Siegert, M. J., Vaughan, D. G., & Corr, HughF. J. (2004). The role of ice thickness and bed properties on the dynamics of the enhanced-flow tributaries of Bailey Ice Stream and Slessor Glacier, East Antarctica. *Annals of Glaciology*, *39*, 366–372. https://doi.org/10.3189/172756404781814375

Rosen, P. a., Hensley, S., Peltzer, G., & Simons, M. (2004). Updated repeat orbit interferometry package released. *Eos, Transactions American Geophysical Union*, *85*(5), 47. https://doi.org/10.1029/2004EO050004

Schellenberger, T., Dunse, T., Kääb, A., Schuler, T. V., Hagen, J. O., & Reijmer, C. H. (2017). Multi-year surface velocities and sea-level rise contribution of the Basin-3 and Basin-2 surges, Austfonna, Svalbard. *The Cryosphere Discussions*, *February*, 1–27. https://doi.org/10.5194/tc-2017-5

Sevestre, H., & Benn, D. I. (2015). Climatic and geometric controls on the global distribution of surge-type glaciers: Implications for a unifying model of surging. *Journal of Glaciology*, *61*(228), 646–662. https://doi.org/10.3189/2015JoG14J136

Sevestre, H., Benn, D. I., Luckman, A., Nuth, C., Kohler, J., Lindbäck, K., & Pettersson, R. (2018). Tidewater glacier surges initiated at the terminus. *Journal of Geophysical Research: Earth Surface*, *123*, 1035–1051. https://doi.org/10.1029/2017JF004358

Shepherd, A., Ivins, E. R., A, G., Barletta, V. R., Bentley, M. J., Bettadpur, S., et al. (2012). A reconciled estimate of ice-sheet mass balance. *Science*, *338*(6111), 1183–1189. https://doi.org/10.1126/science.1228102

Strozzi, T., Kääb, A., & Schellenberger, T. (2017). Frontal destabilization of Stonebreen, Edgeøya, Svalbard. *Cryosphere*, *11*(1), 553–566. https://doi.org/10.5194/tc-11-553-2017

Strozzi, T., Luckman, A., Murray, T., Wegmüller, U., & Werner, C. L. (2002). Glacier-motion estimation, offset tracking SAR, SAR interferometry, surge-type glacier. *IEEE Transactions on Geoscience and Remote Sensing*, *40*(11), 2384–2391. https://doi.org/10.1109/TGRS.2002.805079

Strozzi, T., Paul, F., Wiesmann, A., Schellenberger, T., & Kääb, A. (2017). Circum-Arctic changes in the flow of glaciers and ice caps from satellite SAR data between the 1990s and 2017. *Remote Sensing*, *9*, 947. https://doi.org/10.3390/rs9090947

Truffer, M., & Echelmeyer, K. A. (2003). Of isbræ and ice streams. *Annals of Glaciology*, *36*(1), 66–72. https://doi.org/10.3189/172756403781816347

Tulaczyk, S., Kamb, W. B., & Engelhardt, H. F. (2000). Basal mechanics of Ice Stream B, west Antarctica: 2. Undrained plastic bed model. *Journal of Geophysical Research*, *105*(B1), 483–494. https://doi.org/10.1029/1999JB900328

Van Der Veen, C., & Whillans, I. (1989). Force budget: I. Theory and numerical methods. *Journal of Glaciology*, *35*(119), 53–60. https://doi.org/10.3189/002214389793701581

Weertman, J. (1957). On the sliding of glaciers. *Journal of Glaciology*, *3*, 33–38. https://doi.org/10.3189/S0022143000024709

Wendt, A., Mayer, C., Lambrecht, A., & Floricioiu, D. (2017). A glacier surge of Bivachny Glacier, Pamir Mountains, observed by a time series of high-resolution digital elevation models and glacier velocities. *Remote Sensing*, *9*(4), 388. https://doi.org/10.3390/rs9040388

Willis, M. J., Zheng, W., Durkin, W. J., Pritchard, M. E., Ramage, J. M., Dowdeswell, J. A., et al. (2018). Massive destabilization of an Arctic ice cap. *Earth and Planetary Science Letters*, *502*, 146–155. https://doi.org/10.1016/j.epsl.2018.08.049

Zheng, W., Durkin, W. J., Melkonian, A. K., & Pritchard, M. E. (2019). Cryosphere and remote sensing toolkit (CARST) v1.0.1. https://doi.org/10.5281/zenodo.3475693

Zheng, W., Pritchard, M. E., Willis, M. J., Tepes, P., Gourmelen, N., Benham, T. J., & Dowdeswell, J. A. (2018). Accelerating glacier mass loss on Franz Josef Land, Russian Arctic. *Remote Sensing of Environment*, *211*, 357–375. https://doi.org/10.1016/j.rse.2018.04.004